Studies on preparation and photodynamic mechanism of chlorin P6-13, 15-N-(cyclohexyl)cycloimide (Chlorin-H) and its anti-tumor effect for photodynamic therapy *in vitro* and *in vivo*

Yi-jia Yan, Mei-zhen Zheng, Zhi-long Chen, Xin-hai Yu, Xiao-xia Yang, Zhi-lou Ding, Li Xu

PII: S0968-0896(10)00680-2
DOI: 10.1016/j.bmc.2010.07.027
Reference: BMC 8584

To appear in: *Bioorganic & Medicinal Chemistry*

Received Date: 28 April 2010
Revised Date: 9 July 2010
Accepted Date: 10 July 2010

Please cite this article as: Yan, Y-j., Zheng, M-z., Chen, Z-l., Yu, X-h., Yang, X-x., Ding, Z-l., Xu, L., Studies on preparation and photodynamic mechanism of chlorin P6-13, 15-N-(cyclohexyl)cycloimide (Chlorin-H) and its anti-tumor effect for photodynamic therapy *in vitro* and *in vivo*, *Bioorganic & Medicinal Chemistry* (2010), doi: 10.1016/j.bmc.2010.07.027

***Graphical Abstract**

Studies on preparation and photodynamic mechanism of chlorin P6-13, 15-N-(cyclohexyl)cycloimide (Chlorin-H) and its anti-tumor effect for photodynamic therapy *in vitro* and *in vivo*

Yi-jia Yan, Mei-zhen Zheng, Zhi-long Chen*, Xin-hai Yu, Xiao-xia Yang, Zhi-lou Ding, Li Xu

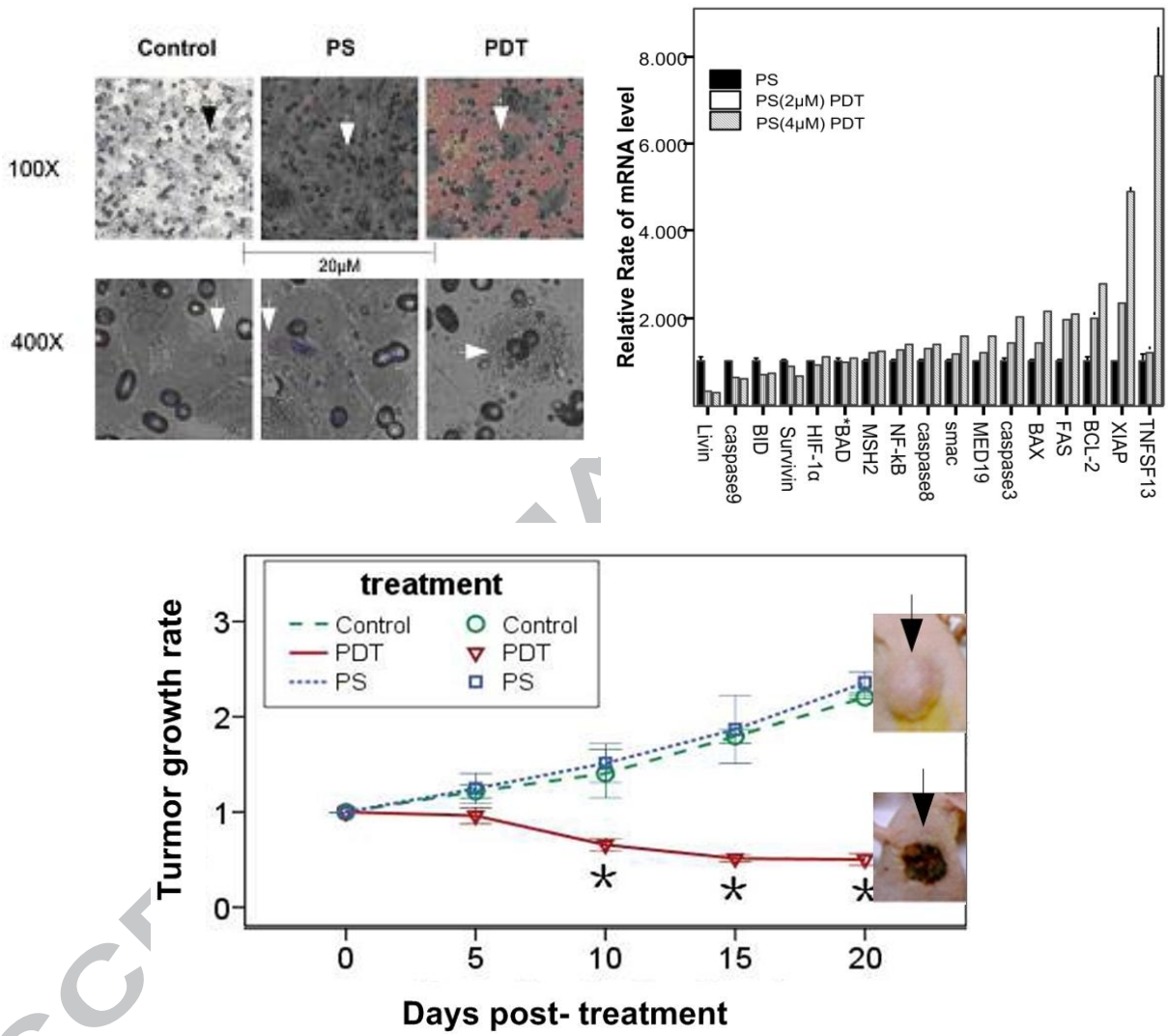

Studies on preparation and photodynamic mechanism of chlorin P6-13, 15-N-(cyclohexyl)cycloimide (Chlorin-H) and its anti-tumor effect for photodynamic therapy *in vitro* and *in vivo*

Yi-jia Yan, Mei-zhen Zheng, Zhi-long Chen*, Xin-hai Yu*, Xiao-xia Yang, Zhi-lou Ding, Li Xu

Department of Pharmaceutical Science & Technology, College of Chemistry and Biology, Donghua University, Shanghai, 201620, China

* Corresponding author: Zhi-long Chen, Department of Pharmaceutical Science & Technology, College of Chemistry and Biology, Donghua University, 2999 North Renmin Road, Shanghai, 201620, P. R. China. Tel (Fax): 86-21-67792654, Email:zlchen1967@yahoo.com

Abstract

Photodynamic therapy (PDT) represents a promising method for treatment of cancerous tumors. The chemical and physical properties of used photosensitizer play key roles in the treatment efficacy. In this study, a novel photosensitizer, Chlorin-H [chlorin P6 - 13, 15-N-(cyclohexyl) cycloimide] which displayed a characteristic long wavelength absorption peak at 698nm was synthesized. Following flash photolysis with 355nm laser, Chlorin-H is potent to react with O_2 and then produce $^1O_2$. This finding indicates that Chlorin-H takes its effects through type II mechanism in PDT. Generally, Chlorin-H is localized in mitochondria and nucleus of cell. After light irradiation with 698nm laser, it can kill many types of cell, inhibit cell proliferation and colony formation, suppress cancer cell invasiveness and trigger apoptosis *via* the mitochondrial pathway in A549 cells *in vitro*. In addition, Chlorin-H-PDT can destroy A549 tumor in nude mice and a necrotic scab was formed eventually. The expression levels of many genes which regulated cell growth and apoptosis were determined by RT-PCR following Chlorin-H-PDT. The results showed that it either increased or decrease. Among which, the expression level of TNFSF13, a member of tumor necrosis factor superfamily, increased significantly. Silencing of TNFSF13 caused by RNA interference decreased the susceptibility of A549 cells to Chlorin-H-PDT. In general, Chlorin-H is an effective antitumor photosensitizer *in vitro* and *in vivo* and is worthy of further study as a new drug candidate. TNFSF13 will be an important molecular target for the discovery of new photosensitizers.

Key Words: Chlorin-H, photosensitizer, photodynamic therapy, cancer, TNFSF13, molecular target

1. Introduction

Photodynamic therapy (PDT) has emerged as a promising new approach for treating and curing cancerous tumors [1]. It takes effect through localization of

photosensitizer (PS) in the target tissues prior to radiation with an appropriate wavelength [2, 3]. PDT has potential advantage over surgery and radiotherapy due to its tissue-sparing properties. However, most of PSs also display only a slight preference for malignant cells, resulting in significant skin photosensitivity and high uptake by healthy cells and tissues. To enhance the treatment of cancer, new PS with absorption spectra at long wavelengths (650-800nm) which can improve tumor selectivity and a quicker clearance are urgently needed to be developed.

Purpurinimides are porphyrin-based aromatic conjugated macrocycles in which the presence of an additional imide ring fused at the *meso*-position extends its long wavelength absorption to 700 and 800 nm [4, 5]. Such an inherent long-wavelength characteristic provides more efficient light penetration in tumor tissues as compared to those photosensitizers absorbing light at short wavelength [6]. Therefore, efforts in our laboratory were directed toward synthesis of chemically pure new longer-wavelength absorbing photosensitizers related to purpurinimides.

In the present study, a novel tetrapyrrole derivative, Chlorin-H, was synthesized and its generation of excited triplet states was investigated.. The localization pattern of Chlorin-H was determined. We further proved that the photodynamic efficacy was determined by the subcellular localization of PS. The photosensitizing antitumor activity *in vitro* and *in vivo* wa evaluated and the induction of apoptosis was measured by Chlorin-H-PDT. To explore the changes in gene expression that occured in response to Chlorin-H-PDT, the expression levels of genes involved in cell apoptosis and growth were analyzed. Furthermore, the role of the target genes in Chlorin-H-PDT was examined via siRNA technology.

2. Material and methods

2.1 Synthesis of Chlorin-H

^{1}H NMR spectra were recorded on a Bruker AVANCE 500-MHz spectrometer with TMS as internal standard. Mass spectrometry (MS) spectra were recorded on a HP 5989A instrument. Ultraviolet spectra were recorded on a Jasco V-530 spectrophotometer using dichloromethane as the solvent. Cyclohexylamine, triethylamine, dichloromethane were used without any purification.

2.1.1 Synthesis of purpurin-18

Purpurin-18 was prepared from silkworm feculae according to reference [7]. Silkworm feculae (150g) were added to the mixture of diethyl ether (1500 ml) and 150 ml propanol containing 20% KOH. The solution was stirred for 1 hour while air was bubbled through it and washed with water three times. 10% H_2SO_4 was added up

until the pH reached 1~2. Then the solution was stirred at the room temperature for 12 hours. For the solution, pH level was adjusted to range from 2~3 by adding aqueous NaOH. The reaction solution was extracted with chloroform and dried over anhydrous Na_2SO_4. The solvent was removed in vacuo to produce black oil residue. The residue was purified by chromatography on silica column using chloroform/methanol (80%) as eluent. A purple solid powder 506 mg was then obtained.

^{1}H NMR(400MHz, δ, $CDCl_3$, ppm): 9.39(1H, s, H10), 9.26(1H, s, H5), 8.55(1H, s, H20), 7.83(1H, dd, J_1=17.6Hz, J_2=11.8Hz, H3^1), 6.27(1H, d, J=17.6Hz, H3^2-CH_2), 6.17(1H, d, J=11.2Hz, H3^2-CH_2), 5.32(1H, s, H17), 4.37(1H, d, J=7.2Hz, H18), 3.65(3H, s, H12^1-CH_3), 3.54(2H, d, J=7.6Hz, H8^1-CH_2), 3.32(3H, s, H2^1-CH_3), 3.10(3H, s, H7^1-CH_3), 2.49(2H, m, H17^1-CH_2), 1.98(2H, m, H17^2-CH_2), 1.61(3H, m, H18^1-CH_3), 1.3(3H, m, H8^2 -CH_3). MS(ESI): 565.3(M+1).

2.1.2 Synthesis of chlorin P6 13,15-N-(cyclohexyl)cycloimide

Cyclohexanamine (0.5ml, 4.4mmol) was added to the solution of purpurin-18 (500mg, 0.89mmol) in chloroform (20 ml). The resulting solution was stirred overnight at room temperature. After the solvent was removed under vacuum, the residue was dissolved in acetic anhydride (3ml) and stirred at 70 °C for 2 hours, then 5% $NaHCO_3$ (20mL) was added and the mixture was stirred for 12 hours. The mixture was extracted with chloroform; the organic layer was dried over anhydrous Na_2SO_4, and then filtered and concentrated under vacumm. The residue was purified by column chromatography on silica gel with chloroform/methanol(65%) as eluent to afford Chlorin-H as purple solid powder 130mg, yield 22.73%[8]. ^{1}H-NMR (400MHz, $CDCl_3$) δ 9.576(s,1H), 9.312(s,1H), 8.579(s,1H), 7.862(dd, J_1=18Hz, J_2=11.6Hz, 1H), 6.23(dd, J_1=18Hz, J_2=11.6Hz, 1H), 6.111(dd, J_1=18Hz, J_2=11.6Hz,1H), 5.392~5.531(m,2H), 4.351(m,1H), 3.814(s,3H), 3.601(m,2H), 3.331(m,3H), 3.216(s,3H), 2.886~2.754(m,3H), 2.416 ~ 2.383(m,3H), 2.068~1.986(m, 2H), 2.060~1.224(m, 6H), 1.645(m,3H), 1.252(m,3H), -0.254(s, 2H). ^{13} C-NMR (100 MHz, $CDCl_3$) δ 178.5, 176.1, 174.1, 168.2, 164.0, 155.0, 149.7, 145.2, 142.4, 139.6, 137.4, 136.6, 136.2, 135.6, 131.8, 130.9, 128.7, 122.8, 116.4, 106.4, 102.3, 98.1, 94.6, 54.7, 53.6, 49.0, 32.1, 31.0, 30.1, 29.9, 29.7, 27.0, 25.7, 24.0, 19.3, 17.4, 12.5, 11.9, 11.0. MS (ESI) *m/z*: 646.3[M+H]$^+$. HRMS calcd for $C_{39}H_{43}N_5O_4$ *m/z* 646.3393 [M+H]$^+$, found 646.3418. Anal. Calcd for $C_{39}H_{43}N_5O_4$: C, 72.53; H, 6.71; N, 10.84. Found: C, 72.66; H, 6.90; N, 10.67

2.1.3 Laser flash photolysis experiment

Chlorin-H was dissolved in CH_3CN. Solution (2 mL) was placed in quartz

cuvettes and bubbled continuously for at least 20 min with high-purity（99.99%）gas (usually N_2 or O_2) before a photolysis.

Nd: YAG excimer laser was used as the pump light source. It provides 355nm pulses with 5ns duration and 80mJ per pulse of maximum energy. In this study, 20-30 mJ per pulse was based on our previous experience. A xenon lamp was employed as detecting light source. The laser and analyzing light beam passed perpendicularly through the quartz cell where the sample solution was. The transmitted light entered a monochromator equipped with an R955 photomultiplier. The output signal from the HP54510B digital oscillograph was transferred to a personal computer for analysis. Based on the relation of the output signal and the concentration of the sample, the laser flash photolysis of the sample was recorded with nanosecond accuracy. The laser flash photolysis (LFP) setup and the details of the experiment were in accordance with the previous description.

2.2 In vitro photosensitizing efficacy

2.2.1 Cell lines and cell culture

PDT was performed on an assortment of cell types: human gastric cancer SGC7901 cells, AGS cells and human colon adenocarcinoma SW480 cells, human pulmonary epithelial type II A549 cells, human lung adenocarcinoma A549 cells, human glioma U87 cells and human promyelocytic leukemia HL60 cells. SGC7901, SW480, AGS, H1299 and HL60 cells were cultured in RPMI-1640 medium (Invitrogen, Carlsbad, CA), whereas A549 and U87 cells were cultured in DMEM medium (Invitrogen, Carlsbad, CA). All media were supplemented with 10% heat-inactivated fetal bovine serum (FBS, BioChrom, Cambridge, UK), 100 units/mL penicillin G (Invitrogen, Carlsbad, CA), and 100μg/mL streptomycin (Invitrogen, Carlsbad, CA). All cells were incubated at 37°C in 5% CO_2 in a humidified incubator.

2.2.2 Phototoxicity studies

Cells were incubated in the dark with different concentrations of Chlorin-H for 24h in complete medium. Prior to irradiation, the incubation medium was replaced with fresh medium without FBS, and the cells were then exposed to laser light with normal wavelength 698nm generated by a diode laser light (Changchun New Industries Optoelectronics Tech. China). The energy of 10mW was verified by a laser power meter (Changchun New Industries Optoelectronics Tech. China).

The MTT assay [9] was used to monitor the cytotoxicity mediated by Chlorin-H-PDT. Briefly, AGS and SW480 cells, which were incubated in media containing 0μM, 4μM, 8μM, 16μM, 32μM or 64μM Chlorin-H for 24h, were

irradiated and the MTT assay was then used to analyze cellular sensitivity. The viability of cells was evaluated by incubating HL60, SGC7901, A549, SW40 and AGS cells with 4μM Chlorin-H for 24h prior to irradiation. All cells were seeded at 2000 cells per well in 96-well plates, each group in triplicate at least, and then incubated in a cell culture incubator with 5% CO2 at 37°C. 5μl MTT (5mg/ml) reagent (Sigma, MO, USA) was added to each well and incubated for 4h at 37°C. At the end of the incubation period, the medium was removed and the formazan complex was solubilized with 100μl DMSO. Absorbance of the complex was measured by with a micro-plate reader (Bio-Rad, California, USA) at a wavelength of 570nm.

To assess colony formation capacity, 200 or 400 A549 cells were retrieved post-PDT, seeded in 6-well plates and cultured at 37°C for 10 days (culture medium was replaced every two days). At the end of the culture period, cells were stained with Giemsa (MBCHEM, New Jersey) and imaged using a digital camera. Colonies containing more than 50 cells were counted using an inverted microscope.

2.2.3 Intracellular localization

U87 cells and A549 cells were grown in 8-wells plates on poly-L-lysine coated coverslips, incubated in the dark at 37℃ with 4μM Chlorin-H for 24h, then rinsed in the medium and incubated with 50nm MitoTracker Green (Invitrogen, Carlsbad, CA) for 30min at 37℃. After washed with PBS, cells was re-incubated with 1mg/ml Hoechst 33258 (Beyotime, Nanjing, China) for 10min at 37°C. Double-stained Cells were imaged under a confocal microscope (LSM 510 META, Carl Zeiss, Göttingen, Germany). Images were analyzed with the LSM Image Browser Version 2.8.

2.2.4 Cell Invasion Assay

The effects of Chlorin-H-PDT on cell invasiveness were examined with the Cell Invasion Assay Kit (CHEMICON International, Billerica, MA) according to the manufacturer's instructions. Briefly, A549 cells were seeded at a density of 1.0×10^5 per insert in serum free medium, and 500μl of 10% FBS medium was added to the outer compartment. After 72h, non-invading cells and the extracellular matrix (ECM) gel were removed; membranes from transwell inserts were then stained using the staining solution and rinsed several times in water. Cells were imaged under a bright-field microscope and quantified by dissolving stained cells in 10% acetic acid, and transferred to a 96-well plate for colorimetric reading of the OD at 570nm.

2.2.5 Cell cycle fractionation by FACS

Post-PDT A549 cells were separated into G_0/G_1 or G_2/M and S cell cycle phase fractions as follows. Cells were washed twice with ice-cold phosphate-buffered saline (PBS) and resuspended in 100μl ice-cold PBS. 900μl 70% ice-cold ethanol was added **to the cells, mixed gently, and then incubated in a -20°C freezer for at least 30min.** Cells were washed once with PBS, resuspended in 500μl PBS, stained with propidium iodide (PI, 50μg/ml) in the presence of RNase (100μg/ml) at room temperature for 30min, and analyzed by fluorescence-activated cell sorting (FACSCalibur, BD**).**

2.2.6 Flow cytometric analysis of apoptosis

Cells were harvested 24h after Chlorin-H-PDT, stained with Annexin V-FITC/PI (Propidium Iodide) Apoptosis detection kit (Nanjing KeyGen Biotech) and FACS sorted (FACSCalibur, BD) to measure cellular apoptosis. The ApoScreen Annexin V Apoptosis detection kit (Annexin V-PE, 7-AAD solution; Southern-Biotech) was used to measure early apoptosis. The cell apoptosis mitochondria membrane potential detection kit (JC-1) was also used. Each kit was used according to the manufacturer's protocol.

2.2.7 Real-time PCR

Total RNA was extracted from cells using Trizol reagent (Invitrogen, Carlsbad, CA) according to the manufacturer's protocol. cDNAs were synthesized using M-MLV reverse transcriptase (Promega) for real-time PCR analysis. Real-time PCR was performed using SYBR Master Mixture (TAKARA, Japan) to measure mRNA levels of selected genes (described in Supplementary Table 1) and to detect Smac, p53 and TNFSF13 after RNA interfering. Data were analyzed using the standard curve analysis method with LightCycler 480 Software (Roche Applied Science).

2.2.8 Lentivirus-mediated siRNA silencing of p53 ,Smac and TNFSF13 in A549 cells

Gene-specific siRNA constructs (p53-siRNA, Smac-siRNA and TNFSF13-siRNA) and a negative control siRNA construct (referred to as NC), were generated by Genechem (Shanghai, China). Lentivirus-mediated RNA interference in A549 cells was performed by Genechem (Shanghai, China). Briefly, A549 cells were infected with p53-siRNA, Smac-siRNA and TNFSF13-siRNA 5 days prior to Chlorin-H-PDT. Cellular survival was measured using an MTT assay as described above**.**

2.3 In vivo photosensitizing efficacy

A total of 18 nude BALB/C mice (9 males and 9 females, weighing 15-20g) were used for the study. The mouse tumor models were set up by subcutaneous injection of

1×10^6 A549 cells in the flank. Experiments were initiated when tumors reached ~1cm in diameter (between 21 and 28 days after tumor injection). The mice were randomly divided into three groups: laser radiation group (6 mice), treatment group (6 mice) receiving 8μM Chlorin-H without laser application, and Chlorin-H + laser radiation group (6 mice) which was given 8μM Chlorin-H followed 24 hours later by laser radiation. The mice were restrained in rat holders and exposed to laser (λ=698nm) with a light dose of 78J/cm^2. Tumor regression was evaluated every five days for 20 days.

2.4 Statistical analysis

One-way ANOVA and the Student's T-test were used to measure differences using the SPSS16.0 software package. Data were reported as mean ± SD and *p* values <0.05 were considered significant.

3. Results

3.1 Synthesis and UV-vis absorption spectrum of Chlorin-H

The new photosensitizer chlorin P6-13, 15-N-(cyclohexyl)cycloimide (Chlorin-H) was derived from plant chlorophyll. Chlorophyll-a in silkworm feculae was reacted with potassium hydroxide and oxygen in propanol, then reacted with sulfuric acid to yield purpurin-18[10]. Chlorin-H was obtained through the reaction of purpurin-18 with cyclohexylamine, then with acetic anhydride (scheme 1). It was purified by colum chromatography with purity ≥ 98% and its structure was confirmed by nuclear magnetic resonance (NMR), mass spectrometer (MS), UV-visible spectroscopy, etc.

The UV-vis absorption spectrum of Chlorin-H was determined in acetone at 0.5 μM. As can be seen, the Chlorin-H had an elevated absorption peak at 698nm (Fig. 1), which should provide more efficient light penetration in tumor tissues as compared to Photofrin, suggesting that Chlorin-H might be an effective photosensitizer.

3.2 Generation of excited triplet states of Chlorin-H

The transient absorption spectra of Chlorin-H (8.5×10^{-6}M) after 355 nm laser flash photolysis in N_2-saturated solution was shown in Fig. 2. The transient species had four strong absorptions at 320, 440, 570 and 730 nm respectively and a photobleaching at 410 nm. The decay of the transient species was recorded in Fig. 3. Most of the transient species decayed after 7μs. The decay kinetics of the absorptions (320, 440, 570 and 730nm) were all quasi-first-order reactions and the rate constants were approximatively equal (Table 1), which indicated that these absorptions were the related absorptions of the Chlorin-H excited state species.

Under O_2-saturated condition, the transient species disappeared quickly, as

recorded in Fig 3. The decay kinetics was also first-rate.

The decay constants of the transient species from Chlorin-H with different concentrations (0.003 to 0.03 mM) were determined (Table 1). It was found that the decay accelerated with rates proportional to their ground state concentrations. This indicated that the triplet states underwent self-quenching.

From a plot of the pseudo-first-order rate constant of the triplet decay versus the ground state concentration, bimolecular rate constant of $5.7\times10^{9}\ M^{-1}\cdot s^{-1}$ for Chlorin-H at 320 nm was calculated for the self-quenching(Fig. 4).

From the intercept, monomolecular rate constant of $1.23\times10^{5}\ s^{-1}$ for Chlorin-H at 320 nm was obtained. So the mechanism of laser flash photolysis of Chlorin-H could be illustrated as follows:

$$T + S \rightarrow 2S + \text{energy},$$

$$T \rightarrow S + \text{energy}.$$

$$M \xrightarrow{h\nu} {}^{1}M^{*} \xrightarrow{ISC} {}^{3}M^{*}$$

$${}^{3}M^{*} + M \rightarrow 2M$$

$${}^{3}M^{*} \rightarrow M + \text{energy}$$

Under O_2-saturated or atmosphere-saturated condition, the decay of Chlorin-H excited state accorded with pseudo-first-order rate reaction. It was postulated that the O_2 concentration in the air was 20% (v/v), and the O_2-saturated concentration was 5×10^{-3}M in MeCN. According to the equation: $k_{obs} = k_0 + k_q [O_2]$, the decay rate constant of $2.4\times10^{9}\ M^{-1}\cdot s^{-1}$ for Chlorin-H and O_2 was obtained.

The excited state of Chlorin-H could react with O_2 after photolysis and $^{1}O_2$ was produced, which proved that Chlorin-H took effects through type II mechanism.

3.3 in vitro studies

3.3.1 Subcellular localization of Chlorin-H

Photodynamic efficacy is principally determined by the subcellular localization of a photosensitizer [11], The localization of Chlorin-H (λ_{max}=698nm) in cancer cells was analyzed by MitoTracker Green and Hoechst 33258 counterstaining. It was found that Chlorin-H initially localized in mitochondria with some accumulation in the nucleus in both U87 human glioma cells and A549 human lung cancer cells (Fig. 5).

3.3.2 Chlorin-H-PDT inhibited A549 cell growth and invasiveness

To determine the efficacy of Chlorin-H-PDT, we compared survival rates among several cell lines AGS, SGC7901, A549, SW480, and HL60. The results showed that PDT with 4μM Chlorin-H for 24h could cause substantial cell death in these cancer,

however HL60 cells showed significant resistance(78.58±6.4% survival) to Chlorin-H-PDT compared to other cell lines (Fig. 6A), which suggested that Chlorin-H had different efficacy to different cancer cell lines and was more effective to solid cancers.

Following by Chlorin-H–PDT, colony formation and cell invasion assay were also conducted in cell line A549 to determine the effect of Chlorin-H-PDT. We found no colonies of 50 cells or greater were observed in cells treated by Chlorin-H-PDT ($p < 0.001$; Fig. 6B), and the invasion index of cells treated by Chlorin-H-PDT also dramatically reduced (15.7 ± 0.8%), compared to the control and PS group (control, 74.9 ± 2.5%; PS, 76.4 ± 3.7%; $p < 0.001$) (Fig. 6C).

3.3.3 Chlorin-H-PDT induced apoptosis in A549 cells

Cell-cycle progression of A549 cells treated with Chlorin-H was assessed by flow cytometry after propidium iodide staining. 4h after PDT treatment, the majority cells were in the G2-M phase (56.07%) compared to 11.07% in PS-treated cultures (Fig. 7).

Furthermore, the Hoechst 33258 nuclear staining showed the condensation of chromatin and the dissociation of the nuclear membrane after 24h following PDT, suggesting apoptotic cell death (Fig. 8A). Apoptosis of all the PDT-treated cells were further confirmed by Annexin V/PI staining (Fig. 8B), which revealed that 75.95±2.42% of cells had undergone apoptosis while only 21.99±1.82% had undergone necrosis.

Annexin-v-PE/7-aad staining 24h after Chlorin-H-PDT (Fig. 8C) further showed that PDT induced a robust early apoptosis response (50.28 ± 1.42%), with comparatively less late apoptosis (7.49±0.60%) and other forms of cell death (25.99±0.43%). Next changes in inner transmembrane potentials of mitochondria in response to Chlorin-H-PDT were monitored by using the JC-1 dye test. A significant loss of mitochondrial membrane potential was induced by PDT (Fig 8D, upper panel). It could be concluded that Chlorin-H-PDT exerted its cytotoxicity by affecting mitochondria and nuclear DNA, disturbing cell cycle progression, and ultimately caused apoptotic cell death.

3.3.4 The changes of gene expression in A549 cells treated by Chlorin-H-PDT

To explore the changes of gene expression after Chlorin-H-PDT, total cellular RNA was harvested from A549 cells after 24h incubation in medium containing 2μM or 4μM Chlorin-H followed by a dose of $0.18 J/cm^2$ light irradiation. The expression levels of genes involved in apoptosis and cell growth were then detected by real-time

PCR assay (Fig. 9). The RNA levels of some genes showed significant dose-dependent changes in Chlorin-PDT treated A549 cells compared to PS-treated.

During Chlorin-H-PDT, some genes involved in apoptosis such as Bcl-2, Smac and X-linked inhibitor of apoptosis (XIAP) were significantly up-regulated, and the tumor necrosis factor superfamily member 13 (TNFSF13) also greatly increased after PDT with the higher dose of Chlorin-H (4μM). Chlorin-H-PDT at the dose of 2μM caused hypoxia-inducible factor-1α (HIF-1α) to be down-regulated, however increasing the dose of Chlorin-H further more could promote HIF-1α expression.

3.3.5 The roles of several genes in A549 cells treated by Chlorin-H-PDT

To determine whether the changes of gene expression induced by Chlorin-H-PDT can affect cell growth, A549 cells were transfected with p53-siRNA via lentivirus vectors and the survival rate with SiRNA-silenced p53 after Chlorin-H-PDT treatment was detected. The results showed although p53 mRNA levels were about 60% reduced in A549 cells(Fig.10A), there didn't appear to be any significant difference between the survival rates of p53-siRNA and NC cells (Fig. 11), which indicated that p53 level was not an important mediator for inhibition of cell growth by Chlorin-H–PDT.

The role of Smac of A549 cells during Chlorin-H–PDT was also investigated in this study. After treatment by Chlorin-H–PDT for 24h, the survival rate of A549 cellstransfected with Smac-siRNA(24.47±0.13%) , which reduced the level of Smac mRNA by 60%(Fig.10C), was higher than that of NC cells (18.80±0.01%), but transfection of Smac-siRNA didn't affect the survival in A549 cells without treatment by Chlorin-H–PDT at the same time(Fig. 12).

In order to determine the role of TNFSF13 in Chlorin-H–PDT, TNFSF13-siRNA was expressed in A549 cells (~60% knock-down efficacy, Fig.10B). Silencing TNFSF13 significantly induced resistance to Chlorin-H-PDT(72.12±0.46%), compared to the controls group(NC, 44.90±0.14%, P=0.003, Fig. 13).

3.4 The efficacy of Chlorin-H-PDT against lung cancer *in vivo*

To determine the effects of Chlorin-H-PDT on lung cancer *in vivo*, 1×10^6A549 cells were injected into the axilla of nude mice to form solid tumors ($1cm^3$ in size). 100μL of 8μM Chlorin-H was then injected into the tail vein and 24h later the tumor was irradiated with 130mW/cm laser light for 10min ($78J/cm^2$). As shown in Fig 9, PDT-treated tumors began to shrink within five days and became dark, hardened and dried over the course of the next 10 days, eventually formed a scab by 20 days after treatment. The normal skin phototoxicity subsided within 4 days. In contrast, the

tumors in PS or control group continued to grow and were significantly larger than in PDT-treated group after 10 days post-treatment (Fig. 14).

4. Discussion

An ideal photosensitizer should have absorption spectra at long wavelengths, which allows deeper tissue penetration and decreases non-specific lesions [1]. For instance, 630nm light penetrates less than 0.5cm whereas 700nm light reaches a depth of near 0.8cm [12]. Chlorin-H can be excited by 698nm light. Both *in vitro* and *in vivo* data supported that Chlorin-H might be an ideal photosensitizer.

The chemical properties of a photosensitizer determine its subcellular localization, which in turn affect the cytotoxicity of photo-activation [13]. Some photosensitizers show a broad distribution, while some may localize more specifically [11]. In generally, the photosensitizers that localize in mitochondria show more effectiveness [14]. We found that Chlorin-H localized primarily in mitochondria and, to a lesser degree, the nucleus. During Chlorin-H-PDT, loss of mitochondrial membrane potential happened, which suggested that oxygen consumption could lead to the increased membrane permeability, membrane depolarization and swelling. Therefore, Chlorin-H-PDT-mediated apoptosis may be triggered via mitochondrial pathway [15, 16].

It was found that the expression of some apoptosis factors including survivin and livin/KIAP were up-regulated significantly during Chlorin-H-PDT, and it potentially contributed to cell apoptosis [17, 18]. Although another IAP gene and XIAP (an inhibitor of caspase-9) dramatically increased, SMAC was also up-regulated, which could interact with XIAP to suppress apoptosis inhibition [19] and then lead to apoptosis eventually. The dose-dependent increase of Bcl-2 was inconsistent with the effect of PDT using phthalocyanine photosensitizer Pc 4 [20]. This difference attributed to the different cellular distributions of photosensitizers. Nuclear factor kB (NF-kB) is a nuclear transcription factor that regulates the expression of a large number of important genes for apoptosis [21]. The activation of NF-kB is regarded as a stress response and has been proved to be activated by Chlorin-H-PDT. MSH2 functioned in DNA repair is increased after Chlorin-H-PDT. Thus, the apoptosis induced by Chlorin-H-PDT is likely the result of an integrative response based on the activation and deactivation of different genes that are critical for growth, apoptosis and DNA repair. When treated by PDT with Chlorin-H, hypoxia-inducible factor-1α (HIF-1α) was down-regulated at the dose of 2μM and up-regulated at the dose of 4μM, which likely increased oxygen consumption through the production of reactive

oxygen species.

TNFSF13, which was not only able to induce apoptosis but also able to stimulate tumor cell growth [22, 23], shows significant dose-dependent increase after Chlorin-H-PDT. Survivin plays an important role in tumor and knocking down, which has shown the sensitivity of drug-resistant to anticancer drugs increases and inhibits cell growth in cancer cells [24, 25]. The results showed that the silencing TNFSF13 by RNA interference significantly increased the expression of survivin and decreased the susceptibility of A549 cells to Chlorin-H-PDT induced death without affecting cell growth. So the silence of TNFSF13 up-regulated the expression of survivin, hence decreased the phototoxicity of Chlorin-H. It could be concluded that the activation of TNFSF13 is required Chlorin-H-PDT induced apoptosis in A549 cells and it may become an important target in the discovery of new photosensitizers for PDT.

5. Conclusions

Chlorin-H with an absorption peak at 698nm took effects through type II mechanism in PDT. It localized primarily in mitochondria in cancer cells. Chlorin-H -PDT caused a rapid and robust apoptosis response in A549 cells and other cancer cell lines, suppressed cancer cell invasiveness, inhibited cell proliferation and colony formation and triggered apoptosis via the mitochondrial pathway *in vitro* when exposed to 698nm laser light irradiation. A549 tumors in nude mice were destroyed and a small scab was formed eventually after Chlorin-H-PDT.

In addtion, the survival and growth of cancer cells in response to Chlorin-H-PDT were first demonstrated, to our knowledge, to be sensitive to TNFSF13 function in a pathway that also involved in survivin expression. Knocking-down TNFSF13 expression rendered A549 cells more resistant to Chlorin-H-PDT-induced death, suggesting the activation of TNFSF13 is required Chlorin-H-PDT induced apoptosis in A549 cells. So Chlorin-H is an effective photosensitizer which is worth further study as a new drug candidate and TNFSF13 may be an important molecular target for in the discovery of new photosensitizers for PDT.

Acknowledgement

This work was supported by National Natural Science Foundation of China (Grant No 30976611), Foundation of Shanghai Municipality of China (Grant No. 10ZZ45, 10DZ0502300, 10ZZ45, 1052nm04900), Foundation of Chinese education Ministry (Grant No.108146) and “111project” (Grant No. B07024-SP0905).

References

1. Huang, Z., et al., Photodynamic therapy for treatment of solid tumors--potential and technical challenges. Technol Cancer Res Treat, 2008. 7(4): p. 309-20.

2. Brown, S.B., Brown, E.A., Walker, I. The present and future role of photodynamic therapy in cancer treatment. Lancet Oncol, 2004. 5:p. 497-508.

3. Pndey, R.K., Goswani, L.N., Chen, Y., et al. Nature: A rich source for developing multifunctional agents. Tumor imaging and Photodynamic therapy. Laser Surg. Med, 2006. 38:p. 445-467.

4. Rungta, A., Zheng, G., Pandey, RK., et al. Purpurinimides as photosensitizers: effect of the presence and position of the substituents in the in vivo photodynamic efficacy. Bioorganic & Medicinal chemistry letters 10. 2000. p:1463-1466.

5. Chen, Y.G., Potter, W.; Pandey, R. K., et al. Bacteriopurpurinimides: Highly stable and potent photosensitizers for photodynamic therapy. J. Med. Chem., 2002. 45: p. 255-258.

6. Wilson, B.C.F., T. J.; Patterson, M. S., An optical fiber-based diffuse reflectance spectrometer for non-invasive investigations of photodynamic sensitizers in ViVo (In future directions and applications in photodynamic therapy). Proc. SPIE Int. Soc. Opt. Eng., 1990(IS6): p. 219-481.

7.Brandis A.S., Kozyrev A.N., Mironov A.F. Tetrahedron, Synthesis and study of chlorin and porphyrin dimers with ether linkage. 1992. 48:p. 6491–6499.

8. Mironov A.F., Ruziev R.D., Lebedeva V.S. Synthesis and Chemical Transformations of N-Hydroxy and N-Hydroxyalkylcycloimides of Chlorin p6. Russian Journal of Bioorganic Chemistry. 2004. 30:p. 466–476.

9. Zheng, M.Z., L.M. Zheng, and Y.X. Zeng, SCC-112 gene is involved in tumor progression and promotes the cell proliferation in G2/M phase. J Cancer Res Clin Oncol, 2008. 134(4): p. 453-62.

10. Chen Zhi-Long, C.J.-R., Zou Yong-Long, WU Yu-Lin, ZENG Xiao-Hua, XU Chun-He, The Synthesis of Chlorophyll Derivatives and Th eir Photosynthetic Activities in Purple Bacteria Reaction Centers. ACTA CHIMICA SINICA, 2001. 59(8): p. 1310-1316.

11. Buytaert, E., et al., Role of endoplasmic reticulum depletion and multidomain proapoptotic BAX and BAK proteins in shaping cell death after hypericin-mediated photodynamic therapy. FASEB J, 2006. 20(6): p. 756-8.

12. Mitra, S. and T.H. Foster, Carbogen breathing significantly enhances the penetration of red light in murine tumours in vivo. Phys Med Biol, 2004. 49(10): p.

1891-904.

13. Pogue, B.W., et al., A photobiological and photophysical-based study of phototoxicity of two chlorins. Cancer Res, 2001. 61(2): p. 717-24.
14. Gryshuk, A.L., et al., In vivo stability and photodynamic efficacy of fluorinated bacteriopurpurinimides derived from bacteriochlorophyll-a. J Med Chem, 2006. 49(6): p. 1874-81.
15. Lam, M., N.L. Oleinick, and A.L. Nieminen, Photodynamic therapy-induced apoptosis in epidermoid carcinoma cells. Reactive oxygen species and mitochondrial inner membrane permeabilization. J Biol Chem, 2001. 276(50): p. 47379-86.
16. Kessel, D. and Y. Luo, Photodynamic therapy: a mitochondrial inducer of apoptosis. Cell Death Differ, 1999. 6(1): p. 28-35.
17. Ferrario, A., et al., Survivin, a member of the inhibitor of apoptosis family, is induced by photodynamic therapy and is a target for improving treatment response. Cancer Res, 2007. 67(10): p. 4989-95.
18. Crnkovic-Mertens, I., et al., The anti-apoptotic livin gene is an important determinant for the apoptotic resistance of non-small cell lung cancer cells. Lung Cancer, 2006. 54(2): p. 135-42.
19. Srinivasula, S.M., et al., A conserved XIAP-interaction motif in caspase-9 and Smac/DIABLO regulates caspase activity and apoptosis. Nature, 2001. 410(6824): p. 112-6.
20. Whitacre, C.M., et al., Photodynamic therapy with the phthalocyanine photosensitizer Pc 4 of SW480 human colon cancer xenografts in athymic mice. Clin Cancer Res, 2000. 6(5): p. 2021-7.
21. Bellarosa, D., et al., Sabarubicin- (MEN 10755) and paclitaxel show different kinetics in nuclear factor-kappaB (NF-kB) activation: effect of parthenolide on their cytotoxicity. Anticancer Res, 2005. 25(3B): p. 2119-28.
22. Roth, W., et al., APRIL, a new member of the tumor necrosis factor family, modulates death ligand-induced apoptosis. Cell Death Differ, 2001. 8(4): p. 403-10.
23. Deshayes, F., et al., Abnormal production of the TNF-homologue APRIL increases the proliferation of human malignant glioblastoma cell lines via a specific receptor. Oncogene, 2004. 23(17): p. 3005-12.
24. Ning, S., et al., siRNA-mediated down-regulation of survivin inhibits bladder cancer cell growth. Int J Oncol, 2004. 25(4): p. 1065-71.

25. Yang, H., et al., Influence of SiRNA targeting survivin on chemosensitivity of H460/cDDP lung cancer cells. J Int Med Res, 2008. 36(4): p. 734-47.

Concentration ($\times 10^{-5}$M)	**Rate constants k ($\times 10^{5}$ $M^{-1}\cdot s^{-1}$)**			
	320 nm	**440 nm**	**570 nm**	**730 nm**
0.34	1.44	2.28	2.21	1.59
0.85	1.71	2.56	2.28	1.68
1.36	2.01	3.01	2.47	2.06
1.87	2.26	3.51	2.58	2.22
2.38	2.62	3.68	2.67	2.37

Table 1. The rate constants (k, $\times 10^{5}$ $M^{-1}\cdot s^{-1}$) of absorptions at 320, 440, 570 and 730 nm of Chlorin-H under N_2.

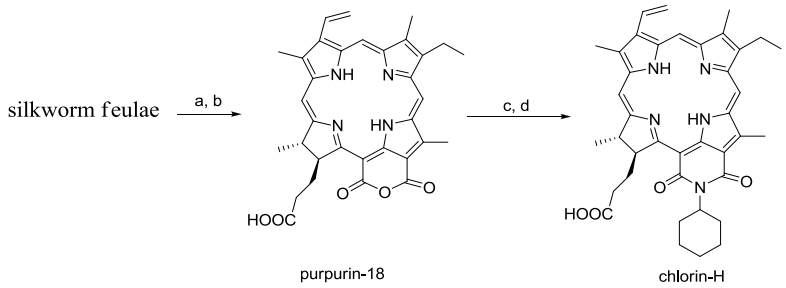

Scheme 1. The preparation and of Chlorin-H. Reagents and conditions: (a) 20% KOH, Propanol, O_2, 1h. (b) 10% H_2SO_4, pH=1~2, 12h. (c) Cyclohexanamine, $CHCl_3$, 12h. (d) Ac_2O, 2h.

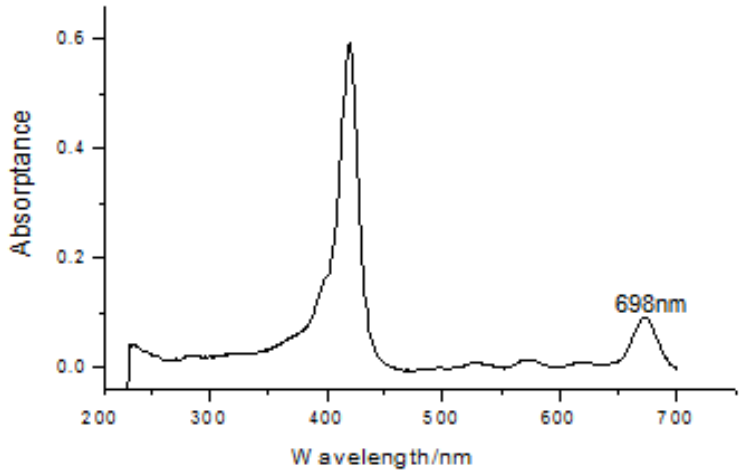

Figure 1. UV-vis spectra of Chlorin-H in acetone at 0.5 μM. Chlorin-H had an elevated absorption peak at 698nm.

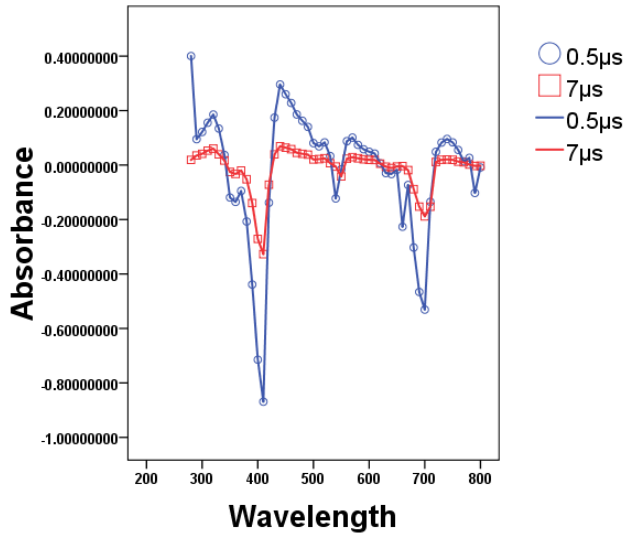

Figure 2. Transient absorption spectra recorded after 355 nm laser flash photolysis of Chlorin-H in N_2-saturated CH_3CN (8.5 μM). (a). at 0.5 μs; (b). at 7 μs.

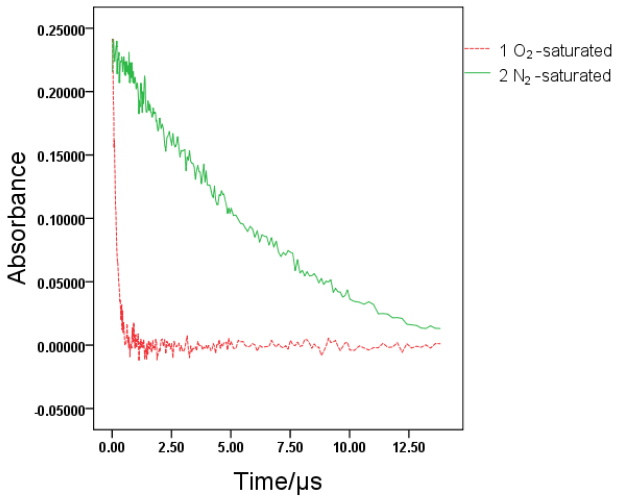

Figure 3. Transient time profile observed at 440 nm in N_2-saturated solution and O_2-saturated solution. (1). in O_2-saturated solution (8.5 μM) (2). in N_2-saturated solution (8.5 μM)

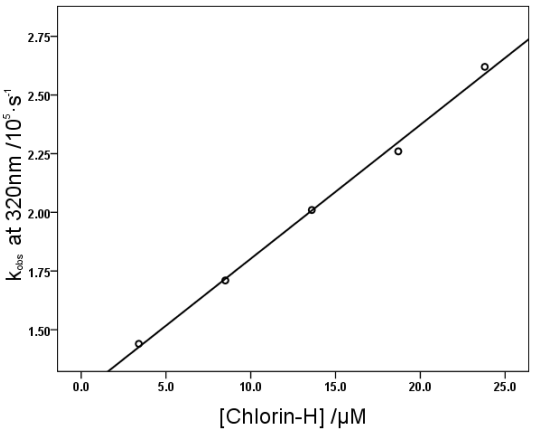

Figure 4. Dependence of the triplet decay rate constant k_{obs} on concentration at 320 nm for Chlorin-H.

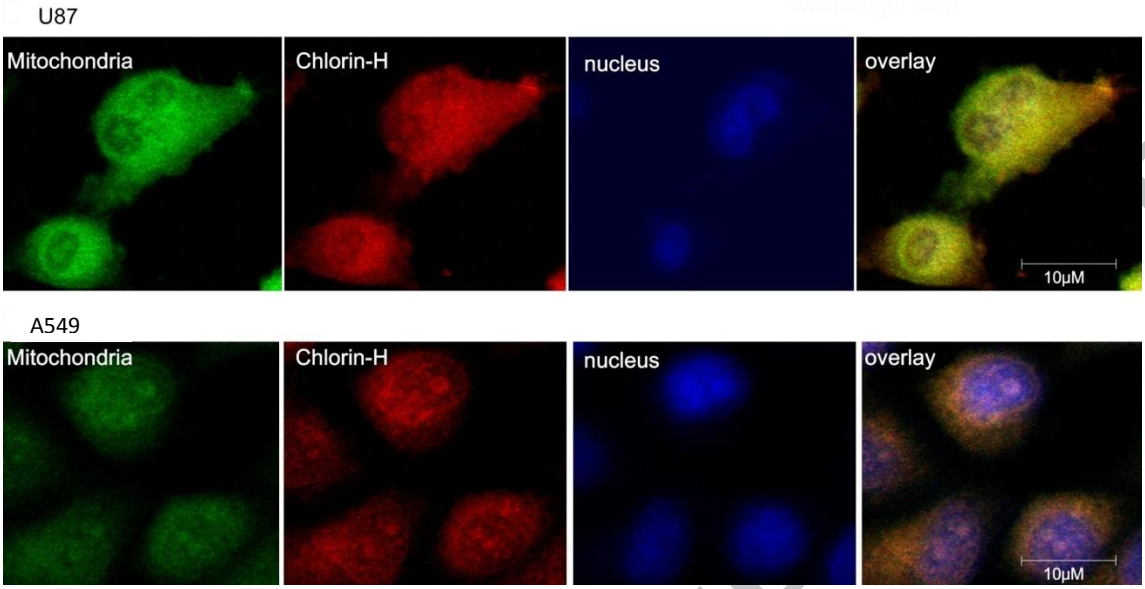

Figure 5. The intracellular localization of Chlorin-H in U87 and A549 cells with MitoTracker Green and Hoechst 33258 respectively. Images were merged to indicate the overlap in fluorescence.

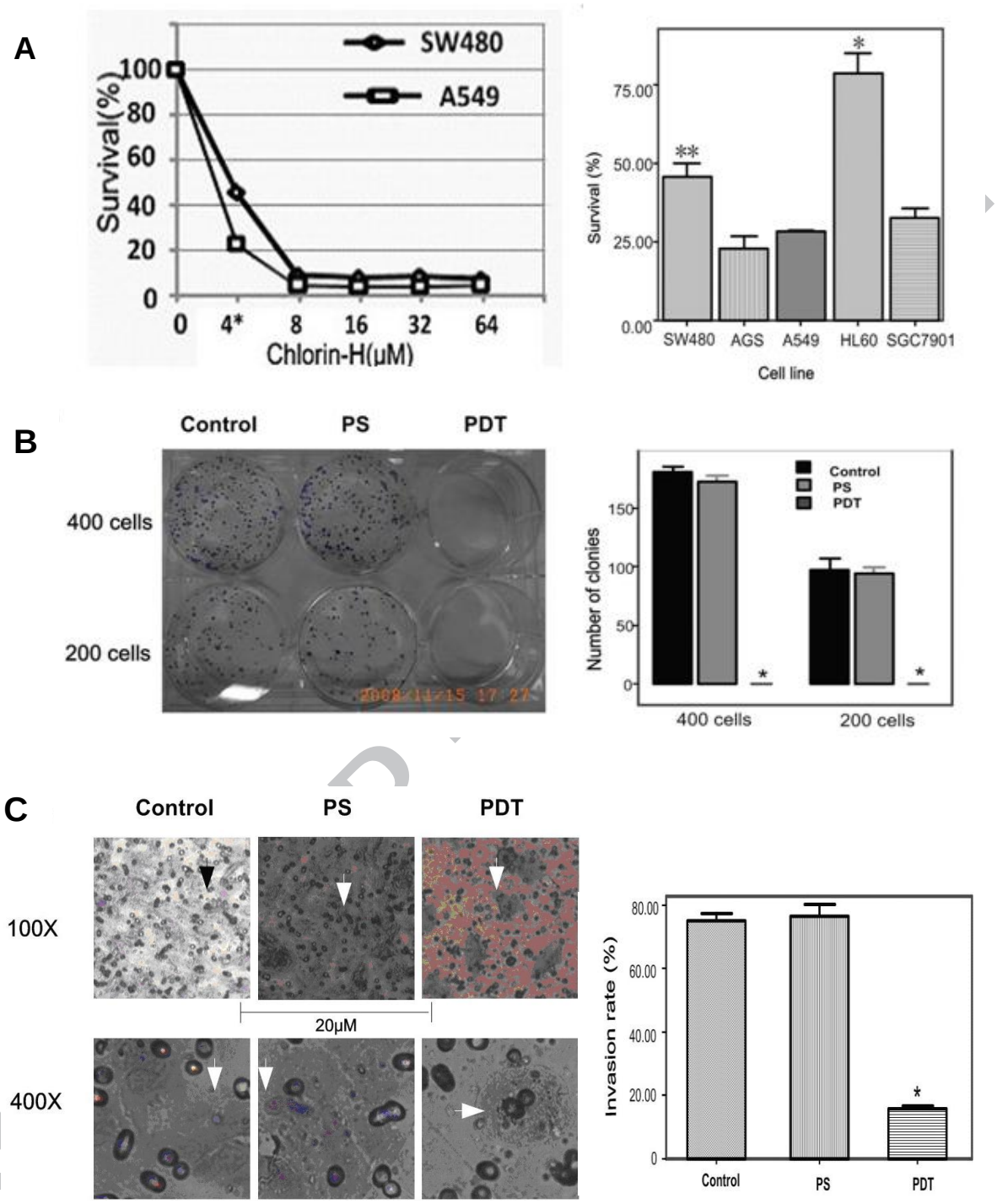

Figure 6. (A). PDT photosensitivity with Chlorin-H (4μM) in various cancer cell lines in vitro at a light dose of 0.18J/cm^2. (B). The effect of Chlorin-H-PDT on cancer proliferation in A549 cells. 14 days after treatment at a 0.18J/cm^2 light dose (control), 24h incubation with 4μM Chlorin-H (PS), or Chlorin-H-PDT (PDT) the number of colonies (>50 cells) were counted (top panel, representative culture dishes; bottom panel, average number of colonies, n=3 per group). (C). The effects of Chlorin-H-PDT on A549 cell invasiveness. Cell migration measured using a Transwell Assay Kit shows the reduced invasive capacity of Chlorin-H-PDT-treated cells (PDT) 72 hours after treatment compared to cells that received a control or PS treatment. *, P < 0.001; **, P<0.05.

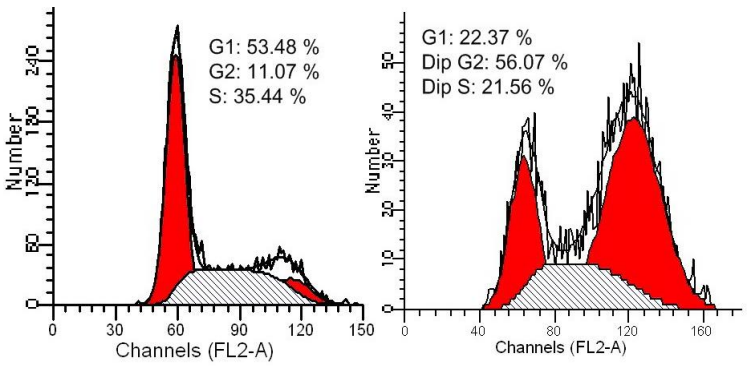

PS **PDT**

Figure 7. The effects of Chlorin-H-PDT on the cell cycle of A549 cells. A549 cells were treated with 4μM Chlorin-H for 24h and then exposed to laser light at 0.18J/cm^2 (PDT) or 4μM Chlorin-H for 24h with no photo-excitation(PS).

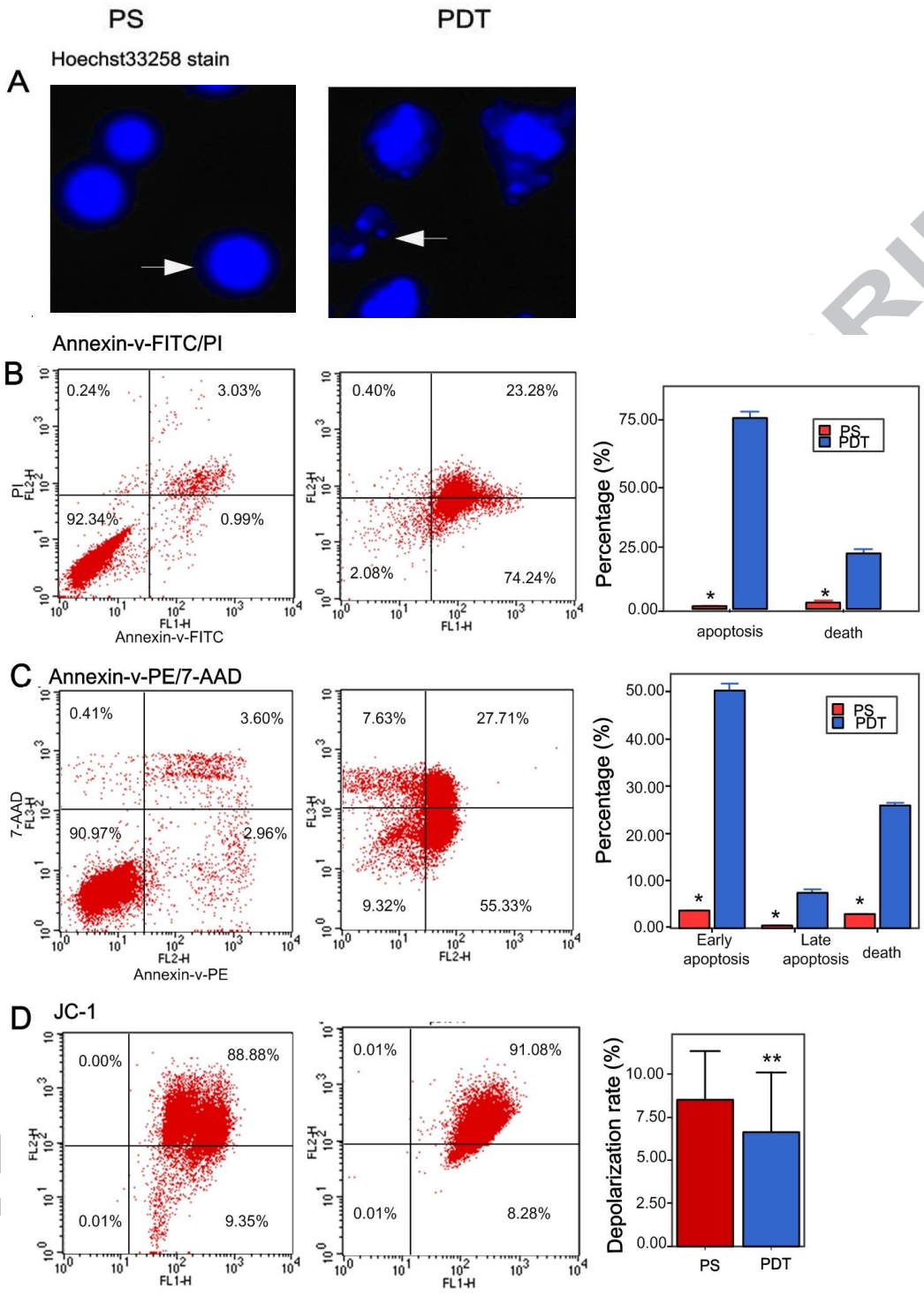

Figure 8. Apoptosis of A549 cells induced by Chlorin-H-PDT. A549 cells were treated with 4μM Chlorin-H for 24h and then exposed to laser light at 0.18J/cm^2 (PDT) or 4μM Chlorin-H for 24h with no photo-excitation(PS). (A). A549 cells were stained with the nuclear label Hoechst 33258, which revealed morphological characteristics of apoptosis in the nucleus, such as chromatin condensation and/or nuclear fragmentation in the PDT group. (B). Annexin-V FITC/PI double stain assay was used to examine apoptosis rates of A549 cells treated by PDT, and apoptosis rates in the

PDT group were significantly higher than that in the PS group ($P < 0.05$). (C). AnnexinV-PE/7-AAD double staining assay also showed apoptosis rates in the PDT group were significantly higher than that in the PS group ($P < 0.05$). (D). Mitochondrial membrane potential was evaluated with JC-1 probe and the results showed that the rate of depolarization in PDT-treated cells was greater than in PS cells group ($P < 0.05$).

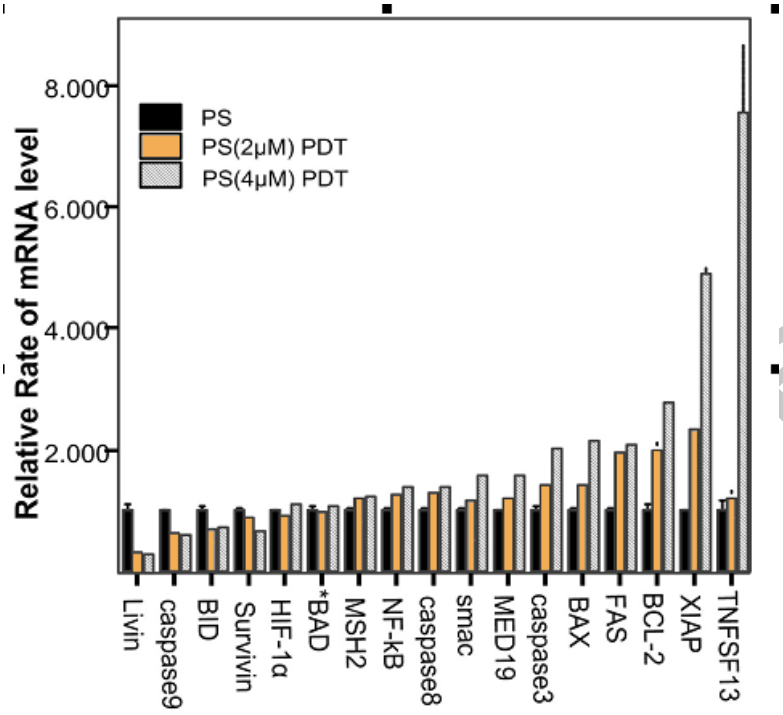

Figure 9. The Changes of gene expression in A549 cells after Chlorin-H-PDT. Real-time PCR results showed the expression changes of 17 genes in A549 cells treated by PDT with 2 or 4μM Chlorin-H, or with 4μM Chlorin-H with no photo-excitation after 24h.

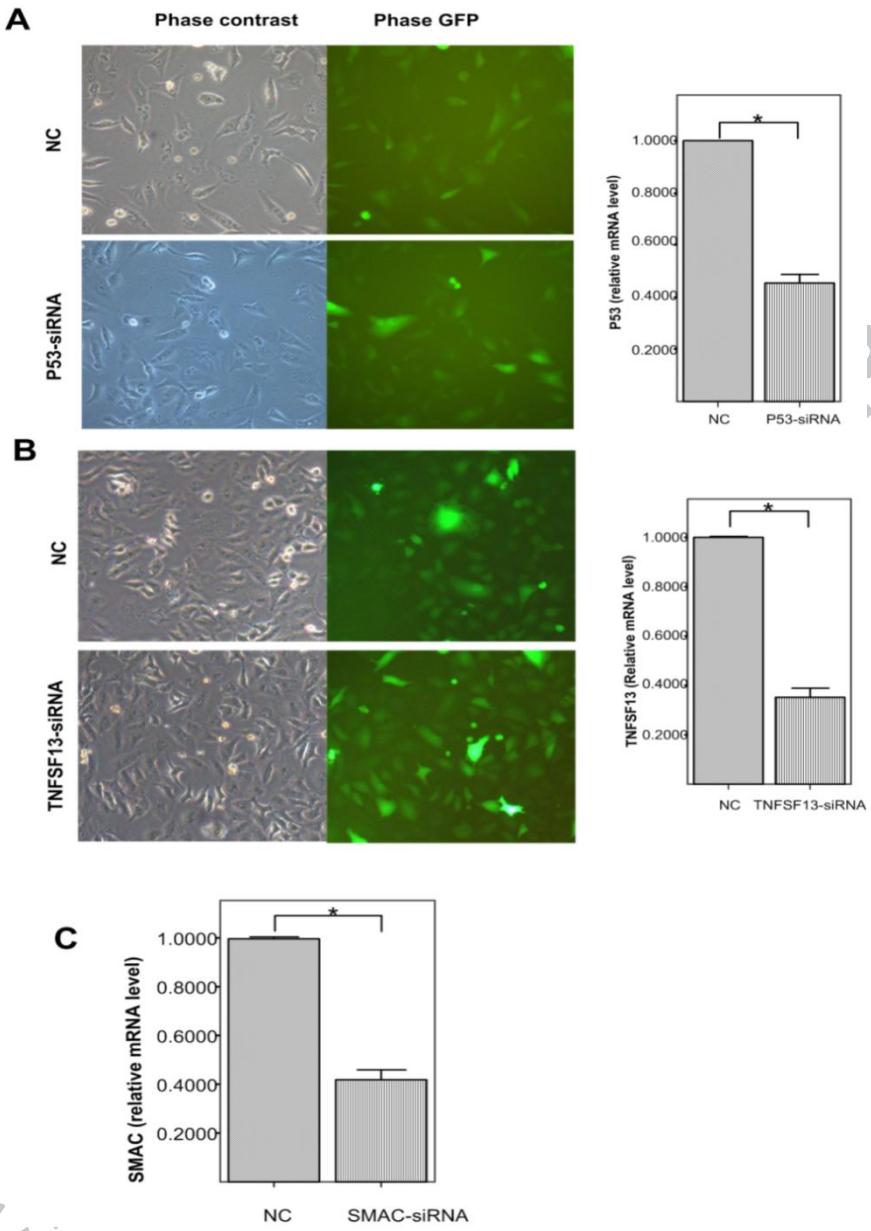

Figure 10. Lentivirus-mediated siRNA knock-down of p53, Smac and TNFSF13 expression in A549 cells. (A). A549 cells transfected with p53-siRNA or NC containing lentivirus particles containing GFP gene were examined by fluorescent microscopy 3 days after transfection. (B). A549 cells transfected with TNFSF13 or NC containing lentivirus particles containing GFP gene were examined by fluorescent microscopy 3 days after transfection. (C). A549 cells transfected with Smac-siRNA or NC containing lentivirus particles containing a puromycin resistance gene were positive selection with 5g/ml puromycin.

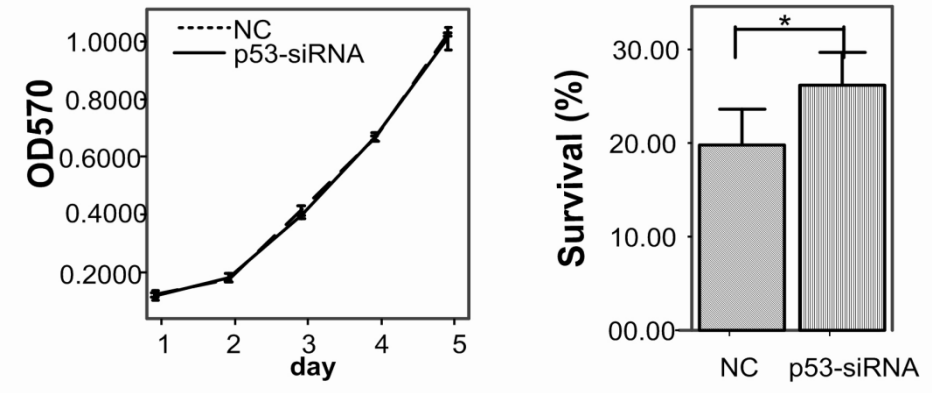

Figure11. After treatment with and without Chlorin-H-PDT, survival of A549 cells , in which p53 expression was suppressed by RNA interference, determined using an MTT assay. p53-siRNA knockdown did not affect post-Chlorin-H-PDT survival of A549 cells. *, P>0.05.

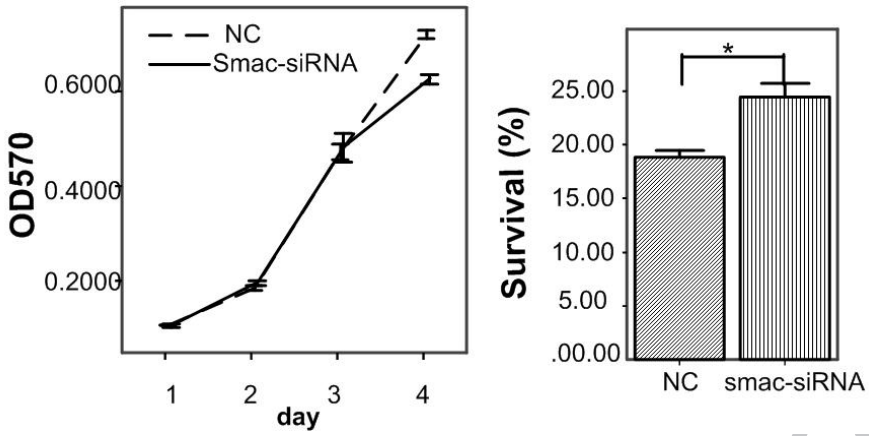

Figure 12. After treatment with and without Chlorin-H-PDT, survival of A549 cells , in which Smac expression was suppressed by RNA interference, determined using an MTT assay. SMAC-siRNA was expressed in A549 cells. Knocking down SMAC significantly increased the resistance of A549 cells to PDT. *, $P<0.05$.

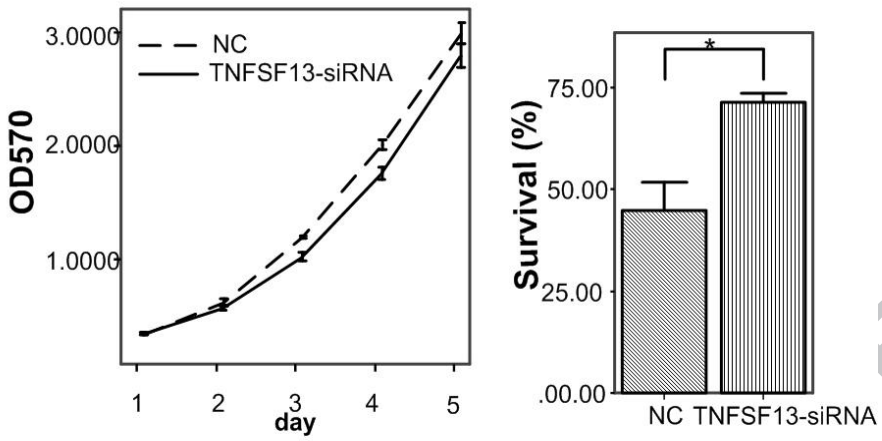

Figure 13. After treatment with and without Chlorin-H-PDT, survival of A549 cells , in which TNFSF 13 expression was suppressed by RNA interference, determined using an MTT assay. Knocking-down TNFSF13 increased the survival of A549 cells following PDT. *, $P < 0.05$.

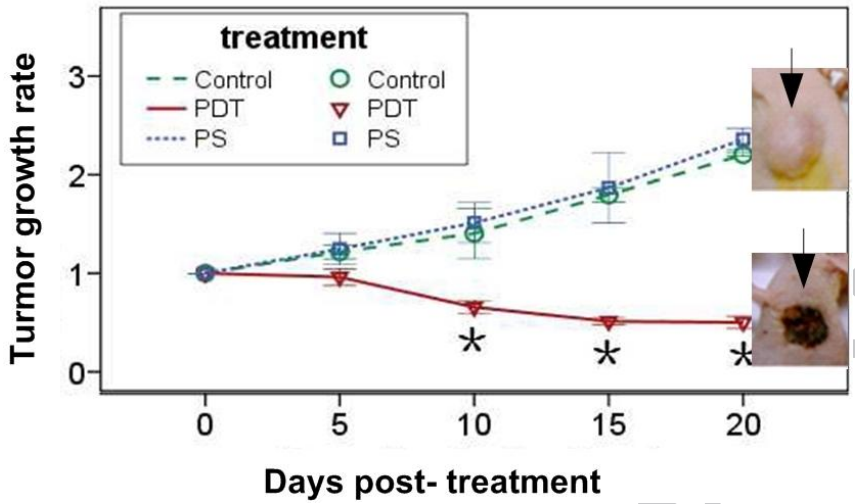

Figure 14. In vivo photosensitizing efficacy of Chlorin-H against lung cancer in nude mice bearing A549 tumors (6 mice/group). The mice in PDT-group were treated with laser light (698 nm, 78J/cm^2) at 24 h postinjection of the drug. The mice in PS-group were treated with 8μM Chlorin-H, but not exposed to light. The control mice were not subjected to any photosensitizer or light.